

# Thermodynamic modeling of spark-ignition engine: Effect of temperature dependent specific heats <sup>☆</sup>

E. Abu-Nada <sup>\*</sup>, I. Al-Hinti, A. Al-Sarkhi, B. Akash

*Department of Mechanical Engineering, Hashemite University, Zarqa, 13115, Jordan*

Available online 18 July 2006

## Abstract

This paper presents thermodynamics analysis of spark-ignition (SI) engine. A theoretical model of air-standard Otto cycle having temperature dependent specific heats has been implemented. It was compared to that which uses constant temperature specific heats. Wide range of engine parameters was studied. In most cases there were significant variations between the results obtained by using temperature dependent specific heats with those obtained at constant specific heats especially at high engine speeds. Therefore, it is more realistic to use temperature dependent specific heat. This should be considered in cycle analysis; especially that temperature variation in the actual cycles is quite large.

© 2006 Elsevier Ltd. All rights reserved.

*Keywords:* Temperature dependent specific heats; SI engine; Otto cycle

## 1. Introduction

In thermal design of the internal combustion engines most researchers use air-standard power cycle models to perform their thermodynamic analyses. Such models are used for comparison reasons in order to show the effect of varying engine parameters, conditions, fluid properties, etc. In most previous studies on air-standard power cycles, air was assumed as the working fluid as an ideal gas with constant specific heats without taking into consideration temperature dependence of the specific heats of the working fluid [1–10]. However, due to the high rise in combustion temperature this assumption becomes less realistic. Although air-standard power cycle analysis gives only approximation to the actual conditions and outputs [11], it would be very useful to compare the performance of air-standard power cycles using constant- and variable-specific heats assumptions. In a recent study the effect of various internal combustion engines parameters in the SI engine were studied [12]. Some studies presented the effect of having temperature dependent specific heats on various air-standard cycles such as Otto, Diesel, and Miller [13–15]. However, the model used for temperature dependent specific heats was a linear model. Constant specific heat models may be used for very small temperature variations. Also, linear models can be applied with moderate temperature changes. However, for large changes in temperature, more accurate models are needed. In this study a more realistic approach on the behavior of variable specific heats will be implemented on the performance evaluation of the SI engine.

<sup>☆</sup> Communicated by W. J. Minkowycz.

<sup>\*</sup> Corresponding author. Fax: +962 5 382 6613.

*E-mail address:* [eyad@hu.edu.jo](mailto:eyad@hu.edu.jo) (E. Abu-Nada).

**Nomenclature**

$A$	Heat transfer area, $m^2$
AF	Air–fuel ratio, dimensionless
$C_p$	Constant pressure specific heat, $kJ/kgK$
$C_v$	Constant volume specific heat, $kJ/kgK$
$D$	Cylinder diameter, $m$
$h_{cg}$	Heat transfer coefficient for gases in the cylinder, $W/m^2K$
$k$	Specific heat ratio, dimensionless
LHV	Lower heating value, $kJ/kg$
$l$	Connecting rod length, $m$
$m$	Mass of cylinder contents, $kg$
$m_f$	Mass of burned fuel, $kg$
$P$	Pressure inside cylinder, $Pa$
$P_i$	Inlet pressure, $Pa$
$Q$	Heat transfer, $kJ$
$Q_{in}$	Heat added from burning fuel, $kJ$
$R$	Crank radius, $m$
$R_g$	Gas constant, $kJ/kgK$
$T$	Gas temperature in the cylinder, $K$
$T_i$	Inlet temperature, $K$
$T_w$	Cylinder temperature, $K$
$U$	Internal energy, $kJ$
$U_p$	Piston speed, $m/s$
$V$	Cylinder volume, $m^3$
$V_c$	Clearance volume, $m^3$
$V_d$	Displacement volume, $m^3$
$x$	Distance from top dead center, $m$
$x_b$	Burning rate of the fuel, dimensionless
$w$	Average cylinder gas velocity, $m/s$
$\theta$	Angle, degree
$\theta_s$	Start of combustion or heat addition, degree
$\Delta\theta$	Duration of combustion, degree

**2. Thermodynamics properties of air**

In most air-standard power cycle models air is assumed to behave as an ideal gas with constant specific heats. The values of specific heats are usually used as cold properties. This assumption can be valid only for small temperature differences. However, the assumption would produce greater error in all air-standard power cycles. In order to account for the large temperature difference encountered in air-standard power cycles, constant average values of specific heats and specific heat ratios are sometimes used. These average values are evaluated using the extreme temperatures of the cycle, and are believed to yield better results. Obviously, this remains a rough simplification and can result in significant deviations from reality. Thus, the incorporation of variable specific heats in air-standard power cycle models can improve their predictions and bring them closer to reality.

One model was introduced by a team of researchers called the NASA polynomial equation [16]. It has the following formula for the temperature range of 200–1000 K:

$$\frac{C_p}{R_g} = 3.56839 - 6.788729 \times 10^{-4} T + 1.5537 \times 10^{-6} T^2 - 3.29937 \times 10^{-12} T^3 - 466.395 \times 10^{-15} T^4 \quad (1a)$$

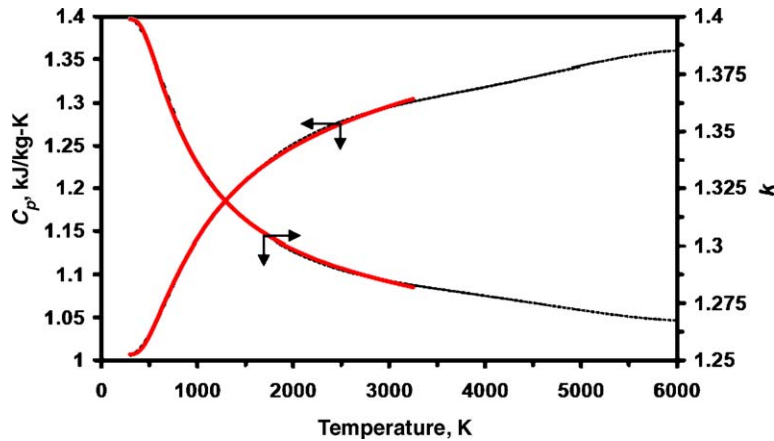


Fig. 1.  $C_p$  and  $k$  versus temperature for air (dotted lines representing Eqs. (1a) and (1b); solid lines representing Eq. (2)).

However, for the temperature range of 1000–6000 K, the above equation is written as:

$$\frac{C_p}{R_g} = 3.08793 + 12.4597 \times 10^{-4} T - 0.42372 \times 10^{-6} T^2 + 67.4775 \times 10^{-12} T^3 - 3.97077 \times 10^{-15} T^4 \quad (1b)$$

Moreover, there is an alternative equation that can be used, except for lower temperature range. It is obtained from Sonntag et al. [17]. It is based on the assumption that air is an ideal gas mixture containing 78.1% nitrogen, 20.95% oxygen, 0.92% argon, and 0.03% carbon dioxide (on mole basis). It is presented in the following equation:

$$C_p = 2.506 \times 10^{-11} T^2 + 1.454 \times 10^{-7} T^{1.5} - 4.246 \times 10^{-7} T + 3.162 \times 10^{-5} T^{0.5} + 1.3303 - 1.512 \times 10^4 T^{-1.5} + 3.063 \times 10^5 T^{-2} - 2.212 \times 10^7 T^{-3} \quad (2)$$

Fig. 1 presents comparisons between plots of Eqs. (1a), (1b) and (2). Eqs. (1a) and (1b) can be applied to a wide temperature range of 200–6000 K. However, Eq. (2) covers lower temperature range of 300–3500 K. It is found from the figure that specific heat at constant pressure increases with temperature from about 1.0 kJ/kg-K at 300 K to about 1.3 kJ/kg-K at about 3000 K. Surely, such difference should be taken into consideration. Similarly, the specific heat ratio,  $k$ , decreases from 1.40 to about 1.28 within the same temperature range.

### 3. Thermodynamic analysis of air-standard Otto cycle

For a closed system, a small change of the process, the first law of thermodynamics is simply written as:

$$\delta Q - \delta W = dU \quad (3)$$

Therefore, by using the definition of work, the first law can be expressed as:

$$\delta Q - PdV = dU \quad (4)$$

For an ideal gas the equation of state is expressed as:

$$PV = mR_g T \quad (5)$$

By differentiating Eq. (5), we can get:

$$PdV + VdP = mR_g dT \quad (6)$$

Also, for an ideal gas with constant specific heats the change in internal energy is expressed as:

$$dU = mC_v dT \quad (7)$$

By substituting Eq. (7) into Eq. (6) then:

$$dU = \frac{C_v}{R_g} (PdV + VdP) \tag{8}$$

By substituting Eq. (8) into Eq. (4),  $dU$  can be eliminated and thus the following equation is obtained:

$$\delta Q - PdV = \frac{C_v}{R_g} (PdV + VdP) \tag{9}$$

Eq. (9) can be rewritten in terms of heat addition and heat loss as:

$$\delta Q_{in} - \delta Q_{loss} - PdV = \frac{C_v}{R_g} (PdV + VdP) \tag{10}$$

The total amount of heat input to the cylinder by combustion of fuel in one cycle is:

$$Q_{in} = m_f LHV \tag{11}$$

The total heat added from the fuel to the system until the crank position reaches angle  $\theta$  is given as:

$$Q(\theta) = Q_{in} x_b \tag{12}$$

Where  $x_b$  is the Weibe function that is used to determine the combustion rate of the fuel and is expressed as:

$$x_b = 1 - \exp\left(-a \left(\frac{\theta - \theta_s}{\Delta\theta}\right)\right) \tag{13}$$

Also, the total amount of heat loss from the system when the crank moves an increment of  $\delta\theta$ :

$$Q_{loss} = \frac{h_{cg} A}{\omega} (T - T_w) \delta\theta \tag{14}$$

By substituting Eqs. (11), (12), (13), and (14) into Eq. (10) followed by differentiation with respect to crank angle ( $\theta$ ), the following equation is obtained:

$$\frac{dp}{d\theta} = \frac{k-1}{V} \left( Q_{in} \frac{dx_b}{d\theta} - \frac{h_{cg} A}{\omega} (T - T_w) \frac{\pi}{180} \right) - k \frac{P}{V} \frac{dV}{d\theta} \tag{15}$$

Where,  $k = C_p / C_v$  and  $R_g = C_p - C_v$ .

Eq. (15) can be solved by using explicit finite difference technique with second order accurate differentiation. The result is given as:

$$p(\theta) = \frac{4}{3} p(\theta-1) - \frac{3}{1} p(\theta-2) + \frac{k-1}{3V} Q_{in} (3x_b(\theta) - 4x_b(\theta-1) + x_b(\theta-2)) - \frac{2k-1}{3} \frac{h_{cg}(\theta)A(\theta)(T-T_w)}{3V} \frac{1}{\omega} - \frac{2kp(\theta-1)}{3V(\theta)} \left( \frac{V(\theta+1) - V(\theta-1)}{2\Delta\theta} \right) \tag{16}$$

Where,  $dP/d\theta$  was expressed as:

$$\frac{dp}{d\theta} = \frac{3P(\theta) - 4P(\theta-1) + P(\theta-2)}{2\Delta\theta} \tag{17}$$

The instantaneous cylinder volume, area, and displacement are given by the slider crank model as [18]:

$$V(\theta) = V_c + \frac{\pi D^2}{4} x(\theta) \quad (18)$$

$$A(\theta) = \frac{\pi D^2}{4} + \frac{\pi DS}{2} [R + 1 - \cos(\theta) + (R^2 - \sin^2(\theta))^{1/2}] \quad (19)$$

$$x(\theta) = (\ell + R) - [R \cos(\theta) + \{\ell^2 - R^2 \sin^2(\theta)\}^{1/2}] \quad (20)$$

Once the pressure is calculated, the temperature of the gases in the cylinder can be calculated using the equation of state as:

$$T = \frac{P(\theta)V(\theta)}{mR_g} \quad (21)$$

The convective heat transfer coefficient in Eq. (15)  $h_{cg}$  is given by the Woschni model as [19,20]:

$$h_{cg} = 3.26D^{-0.2}P^{0.8}T^{-0.55}w^{0.8} \quad (22)$$

Where,  $w$  is the velocity of the burned gas and is given as:

$$w(\theta) = \left( C_1 U_p + C_2 \frac{V_d T_r}{P_r V_r} [P(\theta) - P_m] \right) \quad (23)$$

In the above equation, the displacement volume is  $V_d$ , and  $V_r$ ,  $T_r$ , and  $P_r$  are reference state properties at closing of inlet valve and  $P_m$  is the pressure at same position to get  $P$  without combustion (pressure values in cranking). The values of  $C_1$  and  $C_2$  are given as:

For compression:  $C_1 = 2.28$ ,  $C_2 = 0$  and for combustion and expansion:  $C_1 = 2.28$ ,  $C_2 = 0.00324$ .

Eq. (16) is solved for each crank angle for  $-180 \leq \theta \leq 180$  using a step size  $\delta\theta = 1^\circ$ . The values of  $\theta = \pm 180$  correspond to BDC whereas the value of  $\theta = 0$  corresponds to TDC. The heat addition in Eq. (16) is only valid for  $\theta_s < \theta < (\theta_s + \Delta\theta)$ , i.e., during the period of combustion. In solving Eq. (16), notice that  $k$ ,  $P$ ,  $T$ , and  $h_{cg}$  are coupled, i.e., solution of one of these variables depends on the solution of others. The solution procedure is as follows: The temperature of the gases is first calculated using Eq. (21). Then, the value of the pressure is determined using Eq. (16). Once the value of the pressure is obtained, the temperature dependent properties  $C_p(T)$  is calculated using Eq. (2). The value of  $C_v(T)$  then is determined from the relation  $[C_v(T) = C_p(T) - R]$ . Thereafter, the value of  $k$  is calculated as  $k(T) = C_p(T)/C_v(T)$ . Finally, the heat transfer coefficient is calculated using the Woschni model given by Eq. (22). The mentioned procedure is repeated for each value of  $\theta$  many times until the change between two successive iterations for all variables ( $T$ ,  $P$ ,  $k$ , and  $h_{cg}$ ) is less than  $10^{-4}$ .

Table 1

Engine and operational specifications used in simulation

Fuel	C <sub>8</sub> H <sub>18</sub>
Compression ratio	8.3
Cylinder bore (m)	0.0864
Stroke (m)	0.0674
Connecting rod length (m)	0.13
Crank radius (m)	0.0337
Clearance volume (m <sup>3</sup> )	5.41 × 10 <sup>-5</sup>
Swept volume (m <sup>3</sup> )	3.95 × 10 <sup>-4</sup>
Engine speed (rpm)	2000–5000
Inlet pressure (bar)	1
Equivalence ratio	1
Ignition timing	–25° BTDC
Duration of combustion	70°
Wall temperature (K)	400

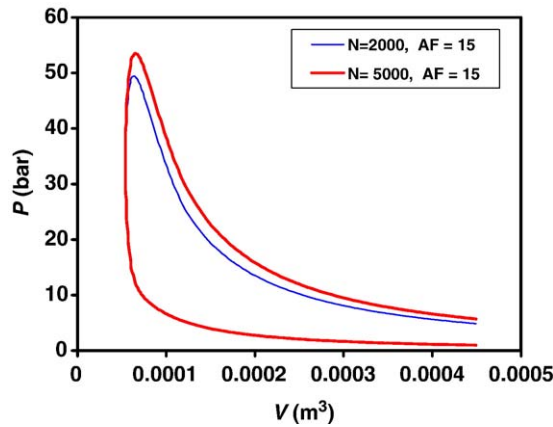


Fig. 2. Variation of cylinder pressure versus volume for SI engine using constant-specific heats running at 2000 rpm and 5000 rpm at air–fuel ratio of 15.

Parametric studies have been performed based on the numerical solution of Eq. (16). The study covers wide range of dependent variables such as engine speed, air–fuel ratio and others, taking into consideration the variation of the specific heat with temperature. Engine specifications, dimensions, and other constants used in the parametric study are listed in Table 1.

#### 4. Results and discussion

In order to examine the validity and sensitivity of the presented model, cylinder pressure is presented in Fig. 2. It shows the variation of cylinder pressure versus volume for SI engine using constant-average specific heats running at piston speeds of 2000 and 5000 rpm at a given air–fuel ratio of 15. It is obvious that cylinder pressure is higher at higher engine speeds. For example, a maximum pressure of 48 and 53 bars is reported at engine speeds of 2000 and 5000 rpm, respectively.

In order to study the effect of temperature dependent specific heats, Fig. 3 is presented. It shows variation of pressure and gas temperature versus crank angle using variable and constant-average specific heats running at engine speed of 5000 rpm and in-cylinder air–fuel ratio of 15. It is obvious that there is some difference when temperature dependent specific heat is used instead of constant specific heat. Although they have similar trends, the maximum temperature and pressure with constant specific heats are significantly over-estimated in comparison with results obtained with variable specific heats.

The effects of engine speed and air–fuel ratios on the gas outlet temperature, using constant and variable specific heat models, are presented in Fig. 4. Fig. 4(a) presents outlet gas temperature versus engine speed at air–fuel ratios of 14 (rich mixture) and 16 (lean mixture). However, Fig. 4(b) presents outlet gas temperature versus air–fuel ratio at engine speeds of 2000 rpm (low speed) and 5000 rpm (high speed). Higher outlet temperatures are obtained at higher engine speeds and lower air–fuel ratios. It is interesting to note that the effect of temperature dependent specific heat is very significant on the gas outlet temperature. Similarly, the effects of engine speed and air–fuel ratios on the maximum gas temperature, using constant and variable specific heat models, are presented in

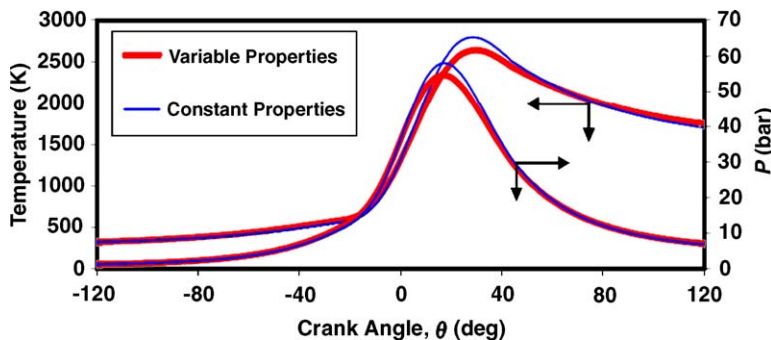


Fig. 3. Variation of gas temperature and cylinder pressure versus crank for SI engine using variable and constant-specific heats running at 5000 rpm and air–fuel ratio of 15.

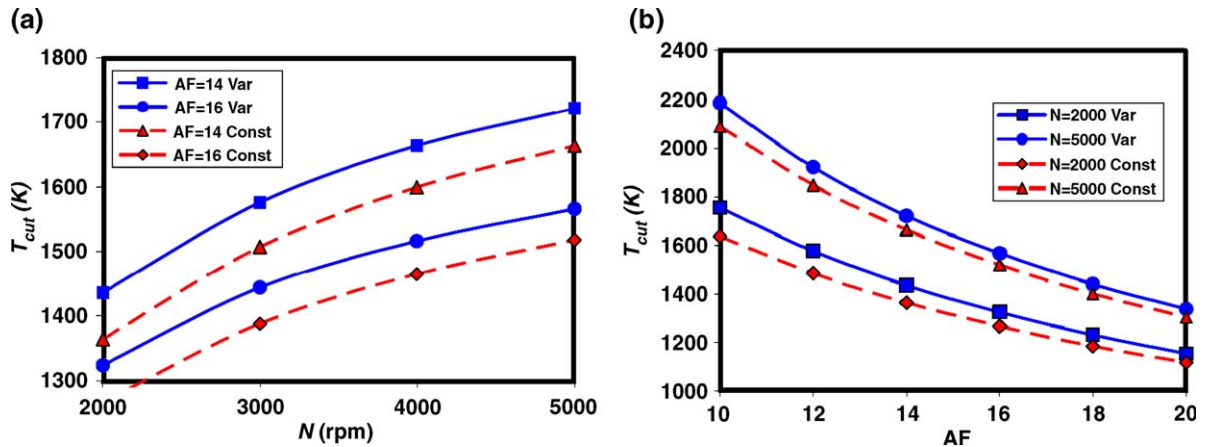


Fig. 4. (a) Outlet gas temperature versus engine speed at different air–fuel ratios using constant and variable specific heat models. (b) Outlet gas temperature versus air–fuel ratio at different engine speeds using constant and variable specific heat models.

Fig. 5. Fig. 5(a) presents the maximum gas temperature versus engine speed at air–fuel ratios of 14 (rich mixture) and 16 (lean mixture). On the other hand, Fig. 5(b) presents maximum gas temperature versus air–fuel ratio at various engine speeds of 2000 rpm (low speed) and 5000 rpm (high speed). Higher values of maximum temperatures are obtained at higher engine speeds and lower air–fuel ratios. Again, as noted previously, the effect of temperature dependent specific heat is very significant on the reported maximum gas temperatures. The effects of engine speed and air–fuel ratios on brake mean effective pressure (BMEP), using constant and variable specific heat models, are presented in Fig. 6(a), which presents BMEP versus air–fuel ratio at engine speeds of 2000 rpm (low speed) and 5000 rpm (high speed). Higher values of BMEP are obtained at higher engine speeds and lower air–fuel ratios. Unlike temperatures, BMEP was not affected significantly with temperature dependent specific heat.

Finally, effect of temperature dependence was investigated on cycle efficiency. The results are presented in Fig. 6(b). It is found that higher thermal efficiencies were produced at higher engine speeds and higher air–fuel ratios. Also, it was found that at low engine speeds using constant or variable specific heat models makes no significant difference on efficiency. However, when the engine runs on high speed it makes a difference whether constant specific heat or variable specific heat models were used; i.e., at higher engine speeds variable specific heat model becomes more considerable.

## 5. Conclusion

It is concluded that engine working parameters are affected by variable specific heats, significantly. The results show that there is a great effect of the temperature dependent specific heat of the working fluid on the performance of the air–

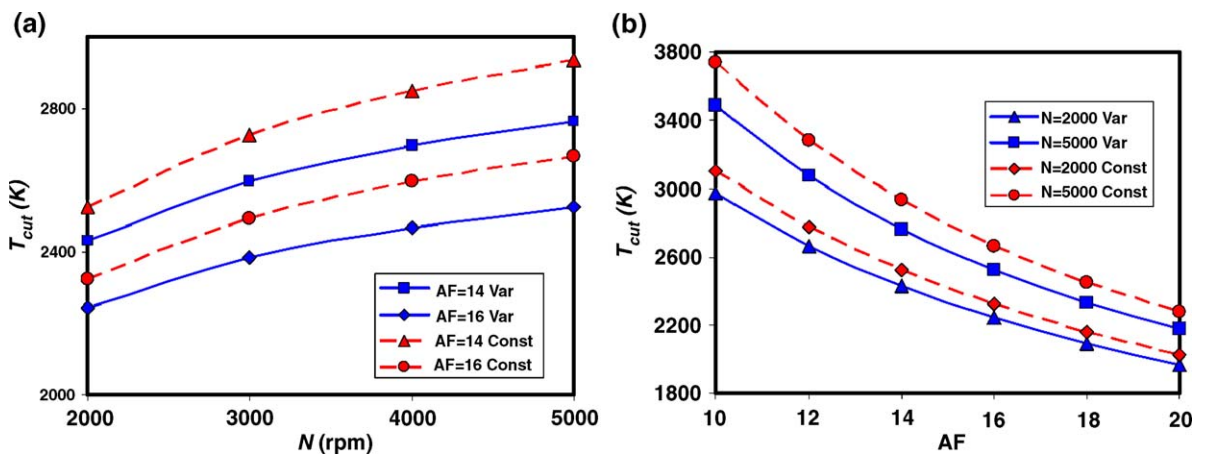


Fig. 5. (a) Maximum gas temperature versus engine speed at different air–fuel ratios using constant and variable specific heat models. (b) Maximum gas temperature versus air–fuel ratio at different engine speeds using constant and variable specific heat models.

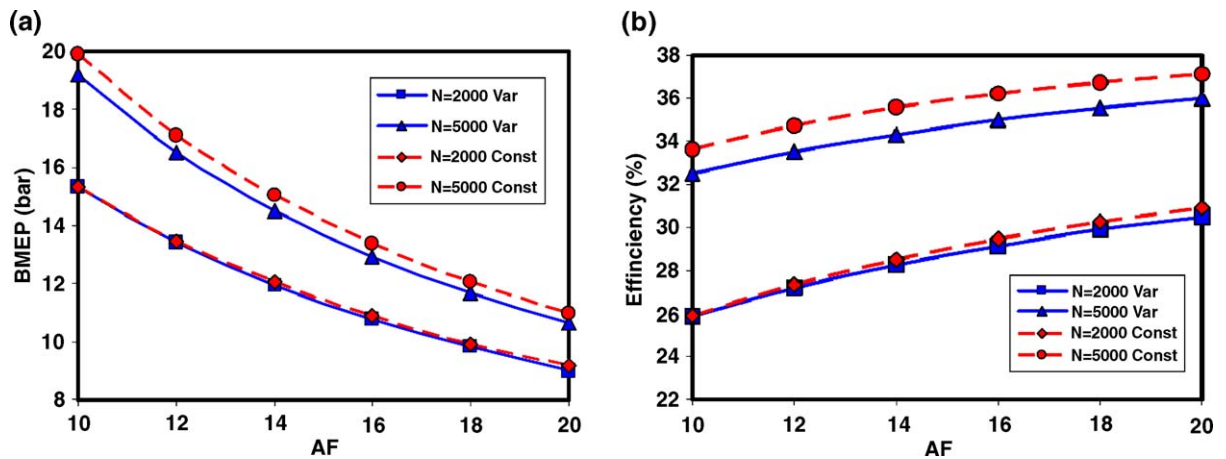


Fig. 6. (a) Brake mean effective pressure versus air–fuel ratio at different engine speeds using constant and variable specific heat models. (b) Efficiency versus air–fuel ratio at different engine speeds using constant and variable specific heat models.

standard Otto cycle. Therefore, it is more realistic to use temperature dependent specific heat during the investigation of air-standard power cycles. This should be considered in the practical cycle analysis, especially, in the actual cycles the temperature variations are quite large. The results are expected to provide significant guidance for the performance evaluation and improvement of real SI engines.

## References

- [1] B. Akash, Effect of heat transfer on the performance of an air-standard diesel cycle, *International Communications in Heat and Mass Transfer* 28 (1) (2001) 87–95.
- [2] A. Al-Sarkhi, B. Akash, J. Jaber, M. Mohsen, E. Abu-Nada, Efficiency of Miller engine at maximum power density, *International Communications in Heat and Mass Transfer* 29 (8) (2002) 1159–1167.
- [3] Y. Ge, L. Chen, F. Sun, C. Wu, Effect of heat transfer and friction on the performance of an irreversible air-standard miller cycle, *International Communications in Heat and Mass Transfer* 32 (2005) 1045–1056.
- [4] L. Chen, C. Wu, F. Sun, S. Cao, Heat transfer effects on the net work output and efficiency characteristics for an air-standard Otto cycle, *Energy Conversion and Management* 39 (1998) 643–648.
- [5] A. Parlak, Comparative performance analysis of irreversible dual and diesel cycles under maximum power conditions, *Energy Conversion and Management* 46 (3) (2005) 351–359.
- [6] A. Parlak, The effect of heat transfer on performance of the diesel cycle and exergy of the exhaust gas stream in a LHR Diesel engine at the optimum injection timing, *Energy Conversion and Management* 46 (2) (2005) 167–179.
- [7] S. Hou, Heat transfer effects on the performance of an air standard dual cycle, *Energy Conversion and Management* 45 (2004) 3003–3015.
- [8] A. Jafari, S. Hannani, Effect of fuel and engine operational characteristics on the heat loss from combustion chamber surfaces of SI engines, *International Communications in Heat and Mass Transfer* 33 (2006) 122–124.
- [9] O. Ozsoysal, Heat loss as a percentage of fuel's energy in air standard Otto and Diesel cycles, *Energy Conversion and Management* 47 (2006) 1051–1062.
- [10] P. Wang, S. Hou, Performance analysis and comparison of an Atkinson cycle coupled to variable temperature heat reservoirs under maximum power and maximum power density conditions, *Energy Conversion and Management* 46 (2005) 2637–2655.
- [11] W. Pulkrabek, *Engineering Fundamentals of the Internal Combustion Engine*, second ed., Pearson Prentice-Hall, Upper Saddle River, New Jersey, 2004.
- [12] M. Karamangil, O. Kaynakli, A. Surmen, Parametric investigation of cylinder and jacket side convective heat transfer coefficients of gasoline engines, *Energy Conversion and Management* 47 (2006) 800–816.
- [13] A. Al-Sarkhi, J. Jaber, M. Abu-Qudais, S. Probert, Effects of friction and temperature-dependent specific-heat of the working fluid on the performance of a diesel-engine, *Applied Energy* 83 (2) (2006) 153–165.
- [14] A. Al-Sarkhi, J. Jaber, S. Probert, Efficiency of a Miller engine, *Applied Energy* 83 (4) (2006) 343–351.
- [15] Y. Ge, L. Chen, F. Sun, C. Wu, Thermodynamic simulation of performance of Otto cycle with heat transfer and variable specific heats of working fluid, *International Journal of Thermal Sciences* 44 (5) (2005) 506–511.
- [16] A. Burcat, B. Ruscic, Third Millennium Ideal Gas and Condensed Phase Thermochemical Database for Combustion with Updates from Active Thermochemical Tables, Argonne National Laboratory, (2005), Report number ANL-05/20, <http://www.chem.leeds.ac.uk/combustion/combustion.html>.

- [17] R. Sonntag, C. Borgnakke, G. Van Wylen, *Fundamentals of Thermodynamics*, fifth ed. Wiley, New York, 1998.
- [18] C. Ferguson, A. Kirkpatrick, *Internal Combustion Engines: Applied Thermosciences*, Wiley, New York, 2001.
- [19] G. Woschni, Universally Applicable Equation for the Instantaneous Heat Transfer Coefficient in Internal Combustion Engine, SAE Paper 670931 (1967).
- [20] R. Stone, *Introduction to Internal Combustion Engines*, third ed., Antony Row, UK, 1999.